Research articles

Spin crossover behavior of a tetranuclear iron(II) grid complex with a hydroxyl-group functionalized multidentate ligand

Takuya Shiga[a,*], Daisuke Ishikawa[a], Minami Tachibana[a], Ryo Saiki[a], Graham N. Newton[b], Hiroki Oshio[a,*]

[a] Graduate School of Pure and Applied Sciences, University of Tsukuba, Tennodai 1-1-1, Tsukuba 305-8571, Japan
[b] GSK Carbon Neutral Laboratories for Sustainable Chemistry, University of Nottingham, Nottingham NG7 2TU, UK

ABSTRACT

A tetranuclear iron grid-type spin crossover complex, $[Fe_4^{II}(HL)_4](BF_4)_4 \cdot 6H_2O$ (**1**) (H_2L = 2-(4-hydroxyphenyl)-4,5-bis{6-(3,5-dimethylpyrazol-1-yl)pyrid-2- yl}-1*H*-imidazole), was synthesized. Magnetic susceptibility measurements revealed that **1** shows gradual spin crossover behavior above 200 K. The electronic states of the compound were elucidated by Mössbauer spectra.

1. Introduction

Spin crossover (SCO) systems attract significant interdisciplinary research interest from molecular and material scientists due to their potential application in molecular switching devices [1]. Iron(II) complexes in which the metal center is held in a ligand field of intermediate strength can exhibit reversible transition between high spin ($S = 2$) and low spin ($S = 0$) states, and significant structural, optical, and magnetic changes accompany the process [2]. The structures and physical properties of mononuclear spin crossover complexes have been extensively studied and molecular design approaches are well-established. In contrast, research into polynuclear spin crossover systems is still in its relative infancy [3,4]. Despite this, the search for single molecular systems with multiple programmable spin states is a key target in molecular electronics [5]. The earliest studies into binuclear SCO systems were reported in 1987 [6], and showed that ligands such as 2,2′-bi-pyrimidine (bpym) could be employed as bridging ligands to connect multiple SCO-active metal centers. Two-step spin crossover behavior was observed for $[Fe(bt)(NCS)_2]_2bpym$ (bt = 2,2′-bi-2-thiazoline), arising from synergistic intramolecular interactions, mediated by the bridging ligand [6b]. More recently, a variety of polynuclear SCO-active clusters have been reported, including tetranuclear cage clusters, $[Fe_4L'_4]^{n+}$ or $[Fe_4L''_6]^{m+}$ (L and L″ are bridging ligands), obtained from the one-pot reaction of iron salts with aldehyde and amine, forming Schiff-base ligands [7]. Octahedral cube-type iron SCO complexes based on imidazolylimine-functionalized porphyrins were constructed, and their host-guest chemistry with fullerenes was investigated [8]. A number of research groups have focused on the fabrication of tetranuclear [2 × 2] grid-type SCO complexes [9–12]. Lehn et al. reported a tetranuclear [2 × 2] grid-type iron(II) SCO complex employing 4,6-bis (2′,2″-bipyrid-6′-yl)-2-phenyl-pyrimidine as a bridging ligand, and found it to exhibit gradual thermal spin transition from 3HS/1LS to 1HS/3LS (HS: high spin, LS: low spin) upon cooling [9]. Sato et al. reported a carbazone-bridged iron(II) [2 × 2] grid complex which showed spin transition from 2HS/2LS to 4HS [10], while Meyer et al. reported two-step SCO behavior in a [2 × 2] grid complex based on polypyridine ligands from 2HS/2LS to 4HS [11]. Our group reported imidazolate bridged tetranuclear [2 × 2] grid complexes showing stepwise SCO behavior (Scheme 1) [12]. $[Fe_4^{II}(L^A)_4](BF_4)_4$ (HL^A = 2-phenyl-4,5-bis[6-(3,5-dimethylpyrazol-1-yl)pyrid-2-yl]-1*H*-imidazole) shows two step SCO in the temperature range of 100–250 K from 2HS-2LS to 4HS [12a] On the other hand, when the ligand was modified with carboxylic acid moieties, the resultant clusters, $[Fe_4^{II}(HL^B)_4](BF_4)_4$ and $[Fe_4^{II}(L^B)_4]$ (H_2L^B = 4-{4,5-bis[6-(3,5-dimethylpyrazol-1-yl)-pyrid-2-yl]-1*H*-imidazol-2-yl} benzoic acid) show one step gradual SCO from 1.5HS/2.5LS to 4HS, and from 4LS to 2HS-2LS, respectively [12c]. These results suggest that modification of peripheral substituents on the bridging ligands can be useful for fine-tuning of the electronic states and SCO behavior of [2 × 2] grid-type complexes.

In the course of developing our research into the magnetic and supramolecular chemistry of polynuclear SCO systems, we are exploring the degree to which ligand modification can be employed to tune the physical properties of the cluster. In this work, a tetranuclear grid complex has been prepared with hydroxyl-group substituents on the
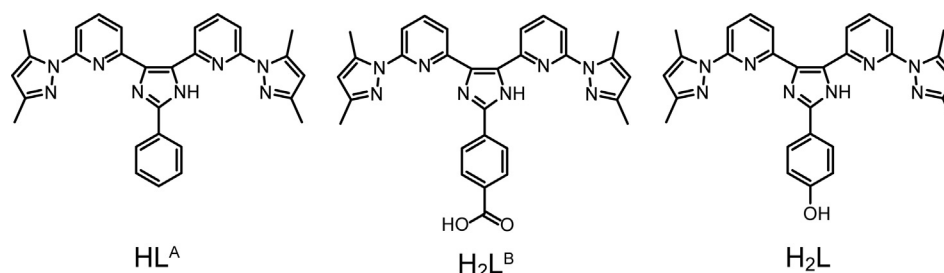
Scheme 1. Three multidentate ligands, HL^A, H_2L^B, and H_2L.

bridging ligands and its supramolecular chemistry and SCO properties have been investigated.

2. Experimental

2.1. Materials

All chemicals were purchased from commercial sources and used without further purification. Bis-{6-(3,5-dimethylpyrazol-1-yl)pyrid-2-yl}glyoxal, which is precursor of the ligand H_2L, was prepared according to the literature method [12a].

2.2. Synthesis of ligand, H_2L (2-(4-hydroxyphenyl)-4,5-bis{6-(3,5-dimethylpyrazol-1-yl)pyrid-2-yl}-1H-imidazole))

Bis-{6-(3,5-dimethylpyrazol-1-yl)pyrid-2-yl}glyoxal (269 mg, 0.673 mmol), 4-hydroxybenzaldehyde (83.3 mg, 0.682 mmol) and ammonium acetate (213 mg, 2.77 mmol) were dissolved in acetic acid (20 cm^3) and refluxed for two hours before cold water was added and the mixture was neutralized by addition of saturated sodium hydrogen carbonate solution. The resulting mixture was extracted into dichloromethane, and the organic phase was dried over anhydrous magnesium sulfate. The solvent was removed in vacuo, and the residue was washed by ethyl acetate/*n*-hexane (1:3) solution to give H_2L (280 mg, 0.557 mmol, 83% yield) as a white solid. ^{1}H NMR (CDCl$_3$) δ 10.7 (s, 1H), 8.33 (d, 1H, J = 8.0 Hz), 8.01 (dd, 1H, J = 8.0 Hz), 7.94 (dd, 1H, J = 8.0 Hz), 7.89 (d, 2H, J = 8.0 Hz), 7.80 (d, 1H, J = 8.0 Hz), 7.68 (dd, 1H, J = 8.0 Hz), 7.59 (d, 1H, J = 8.0 Hz), 6.96 (d, 2H, J = 8.0 Hz), 6.11 (s, 1H), 5.97 (s, 1H), 2.73 (s, 3H), 2.36 (s, 3H), 2.35 (s, 6H). Anal. Found (calc.) for C$_{29}$H$_{30}$N$_8$O$_2$ (H_2L·2H$_2$O): C, 64.93 (64.67); H, 5.61 (5.63); N, 20.70 (20.80) %. IR (KBr pellet, cm^{-1}): 1595, 1568, 1458. ESI–MS m/z (obs.) = 503.23 [H_2L + H$^+$], 525.22 [H_2L + Na$^+$].

2.3. Synthesis of $[Fe_4^{II}(HL)_4](BF_4)_4$·6H$_2$O (1)

A solution of H_2L (31.5 mg, 0.0627 mmol) and trimethylamine (18.2 μL, 0.129 mmol) in acetonitrile (5 ml) was added to Fe(BF$_4$)$_2$·6H$_2$O (21.9 mg, 0.0649 mmol) in acetonitrile (2 ml) and the mixture was stirred for a few minutes with heating. The resulting dark red solution was filtered and *o*-xylene was allowed to diffuse into the filtrate. After a few days, dark red block crystals were obtained. Crystals of [Fe$_4$(HL)$_4$](BF$_4$)$_4$·5H$_2$O suitable for single crystal X-ray structural analysis were collected by filtration (15.2 mg, 0.00455 mmol, 29% yield). An air-dried sample, [Fe$_4$(HL)$_4$](BF$_4$)$_4$·6H$_2$O (1), was used for the physical property measurements. Anal. Found (calc.) for C$_{116}$H$_{110}$N$_{32}$O$_9$B$_4$F$_{16}$Fe$_4$ ([Fe$_4$(HL)$_4$](BF$_4$)$_4$·6H$_2$O): C, 52.05 (51.89); H, 4.13 (4.20); N, 16.48 (16.69) %. IR (KBr pellet, cm^{-1}): 1607, 1557, 1474.

2.4. Physical measurements

Magnetic susceptibility data were collected in the temperature range of 5–400 K in an applied field of 20,000 Oe by using a Quantum Design model MPMS-5XL SQUID magnetometer by using quartz glass sample tube. Pascal's constants were used to determine the diamagnetic corrections.

2.5. X-ray crystallography

Dark red block of 1 (0.30 × 0.20 × 0.20 mm^3) was mounted on the tip of a glass fiber with epoxy resin. Diffraction data were collected at 100 K on a Bruker SMART APEXII diffractometer with a CCD type area detector, and a full sphere of data were collected using graphite-monochromated Mo–K$_\alpha$ radiation (λ = 0.71073 Å). The data frames were integrated using SAINT and were merged to give a unique data set for structure determination. The structures were solved by direct methods and refined by the full-matrix least-squares method on all F^2 data using the SHELXTL package (Bruker Analytical X-ray Systems). Hydrogen atoms were included in calculated positions and refined with isotropic thermal parameters riding on those of the parent atoms.

Crystallographic data for 1 have been deposited at the Cambridge Crystallographic Data Centre as the publication citation and deposition numbers CCDC 1877460. Copies of the data can be obtained free of charge on application to CCDC, 12 Union Road, Cambridge CB21EZ, UK, fax: (+44)1223-336-033; e-mail: deposit@ccdc.cam.ac.uk). A summary of the crystallographic parameters and data is given in Table 1.

Table 1
Crystallographic data for complex 1.

| Compound	1
Formula	C$_{116}$H$_{100}$N$_{32}$O$_4$B$_4$F$_{16}$Fe$_4$
Formula weight	2576.91
Crystal color	Dark red
Crystal habit	Block
Crystal size/mm^3	0.30 × 0.20 × 0.20
Crystal system	Tetragonal
Space group	$P4/ncc$
Unit cell dimensions	
a/Å	20.7815(13)
b/Å	20.7815(13)
c/Å	26.6601(17)
α/°	–
β/°	–
γ/°	–
V/Å^3	11513.7(16)
Z	4
D_{calc}/Mg m^{-3}	1.487
Absorption coefficient/mm^{-1}	0.589
θ range/°	1.242 to 27.497
Reflections collected	63,471
Independent reflections (R_{int})	6620 (0.0357)
Final R indices [$I > 2\sigma(I)$]	$R1$ = 0.0714
	$wR2$ = 0.2047
R indices (all data)	$R1$ = 0.1025
	$wR2$ = 0.2189
Goodness of fit on F^2	1.382
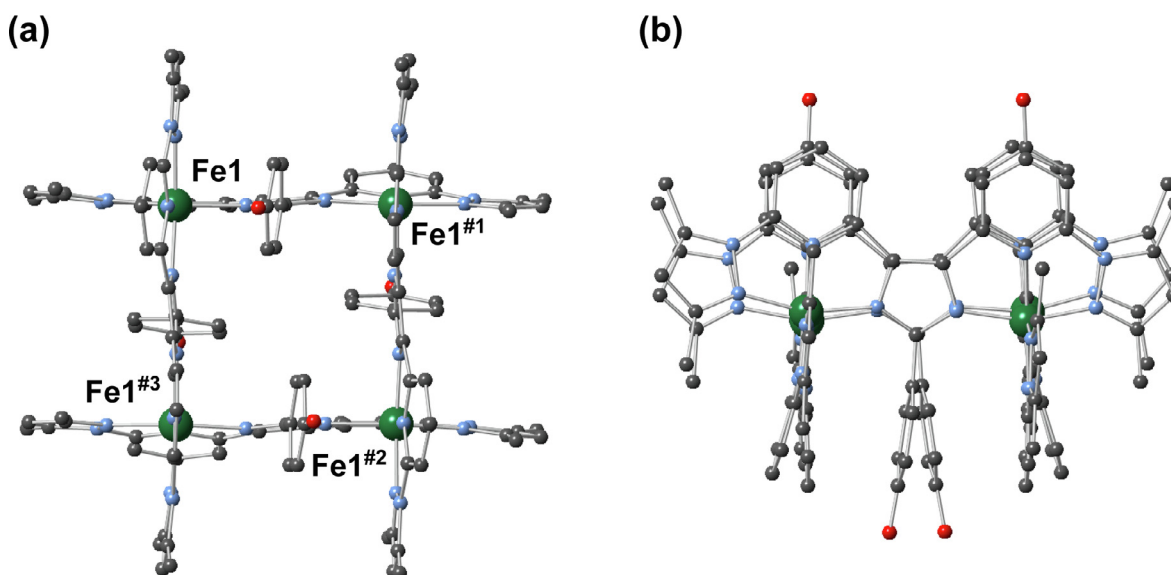
Fig. 1. Molecular structure of **1**. (a) top view, (b) side view. Counter anions and solvent molecules were omitted for clarity. Color code: C, grey; N, light blue; Fe^{II}(LS), green.

3. Result and discussion

3.1. Crystal structures

1 crystallized in the tetragonal space group *P4/nnc* (Fig. 1) and selected atomic separations and bond angles are presented in Table 2. This structure has high symmetry, and the asymmetric constitutes one quarter of the grid molecule. We previously reported three ferrous tetranuclear grid complexes, $[Fe_4^{II}(L^A)_4](BF_4)_4$, $[Fe_4^{II}(HL^B)_4](BF_4)_4$ and $[Fe_4^{II}(L^B)_4]$, which has $P\bar{1}$, $P\bar{1}$, and $P2_1/n$ space groups. The asymmetric unit in each of these examples incorporates one entire grid complex. Considering coordination charge balance, bond lengths and coordination geometry, the electronic state of iron ion at 100 K can be assigned as divalent low spin. The average coordination bond length is 1.966 Å. The Σ value of the iron ion, which corresponds to the sum of the deviation of each of the 12 *cis* N-Fe-N angles from 90°, is 86.07°, which is in the range expected of low spin Fe(II) species [13]. Each grid molecule interacts with its neighbors through hydrogen bonds between water molecules and ligand hydroxyl groups, forming a one-dimensional network elongated along the *c*-axis (Fig. 2).

Table 2
Selected interatomic distances (Å) and angles (°) for complex **1**.

	1
Fe(1)-N(3)	1.906(3)
Fe(1)-N(6)	1.917(3)
Fe(1)-O(8)	1.982(3)
Fe(1)-O(1)	1.987(3)
Fe(1)-O(4)	1.997(3)
Fe(1)-O(5)	2.004(3)
N(3)-Fe(1)-N(8)	99.49(12)
N(6)-Fe(1)-N(8)	80.44(12)
N(3)-Fe(1)-N(1)	80.43(13)
N(6)-Fe(1)-N(1)	98.89(13)
N(8)-Fe(1)-N(1)	88.78(11)
N(3)-Fe(1)-N(4)	80.20(12)
N(6)-Fe(1)-N(4)	100.48(11)
N(8)-Fe(1)-N(4)	91.35(10)
N(3)-Fe(1)-N(1)	99.78(11)
N(6)-Fe(1)-N(5)	80.27(11)
N(1)-Fe(1)-N(5)	93.04(11)
N(4)-Fe(1)-N(5)	93.29(10)

3.2. Magnetic properties

Magnetic susceptibility measurements were performed in the temperature range of 5–400 K and the results are shown in the $\chi_m T$ vs. *T* plot (Fig. 3). The $\chi_m T$ value for **1** is 0.093 emu mol^{-1} K at 5 K, which suggests it is in a diamagnetic state derived from four low spin iron(II) ions. Increasing the temperature led to increases in the $\chi_m T$ values above 200 K, reaching a maximum value of 12.41 emu mol^{-1} K at 400 K. There is an inflection point around 330 K, which may indicate the existence of an intermediate spin state corresponding to 2HS/2LS. The maximum $\chi_m T$ value at 400 K is close to the theoretical value, 12.00 emu mol^{-1} K expected from four high spin iron(II) ions ($S = 2$, $g = 2.00$). This temperature dependent magnetic susceptibility suggests that **1** shows thermal SCO behavior from four low spin iron(II) to four high spin iron(II) ions. The previously reported tetranuclear iron(II) grid complexes show significantly different SCO behavior. $[Fe_4^{II}(L^A)_4]$ $(BF_4)_4$ shows two step SCO in the temperature range of 100–250 K from 2HS/2LS to 4HS states [12a]. While $[Fe_4^{II}(HL^B)_4](BF_4)_4$ and $[Fe_4^{II}(L^B)_4]$ show gradual one-step SCO from 1.5HS/2.5LS to 4HS, and from 4LS to 2HS-2LS, respectively [12c]. The coordination environments in the three complexes are similar, but the spin states were different. This is likely to originate from structural changes to the iron coordination geometry due to intermolecular interactions and packing effects.

4. Mössbauer spectra

In order to elucidate the electronic states of iron ions, the Mössbauer spectrum of **1** was collected at 20 K (Fig. 4). The spectrum was fitted to a doublet, yielding best fit parameters of $\delta_{IS} = 0.39$ mm sec^{-1}, $\Delta E_Q = 0.67$ mm sec^{-1}, which are close to the values of previously reported in similar complexes [12]. The parameters are reasonable values for low spin iron(II) species.

5. Conclusion

A tetranuclear iron grid-type spin crossover complex, $[Fe_4^{II}(HL)_4]$ $(BF_4)_4 \cdot 6H_2O$ **(1)** (H$_2$L = 2-(4-hydroxyphenyl)-4,5-bis{6-(3,5-di-methylpyrazol-1-yl)pyrid-2-yl}-1*H*-imidazole), was synthesized. Magnetic susceptibility measurements revealed that **1** showed gradual spin crossover behavior between 0LS and 4HS states above 200 K. The low temperature electronic structure was confirmed by Mössbauer spectra. These results show how minor modifications to the ligand
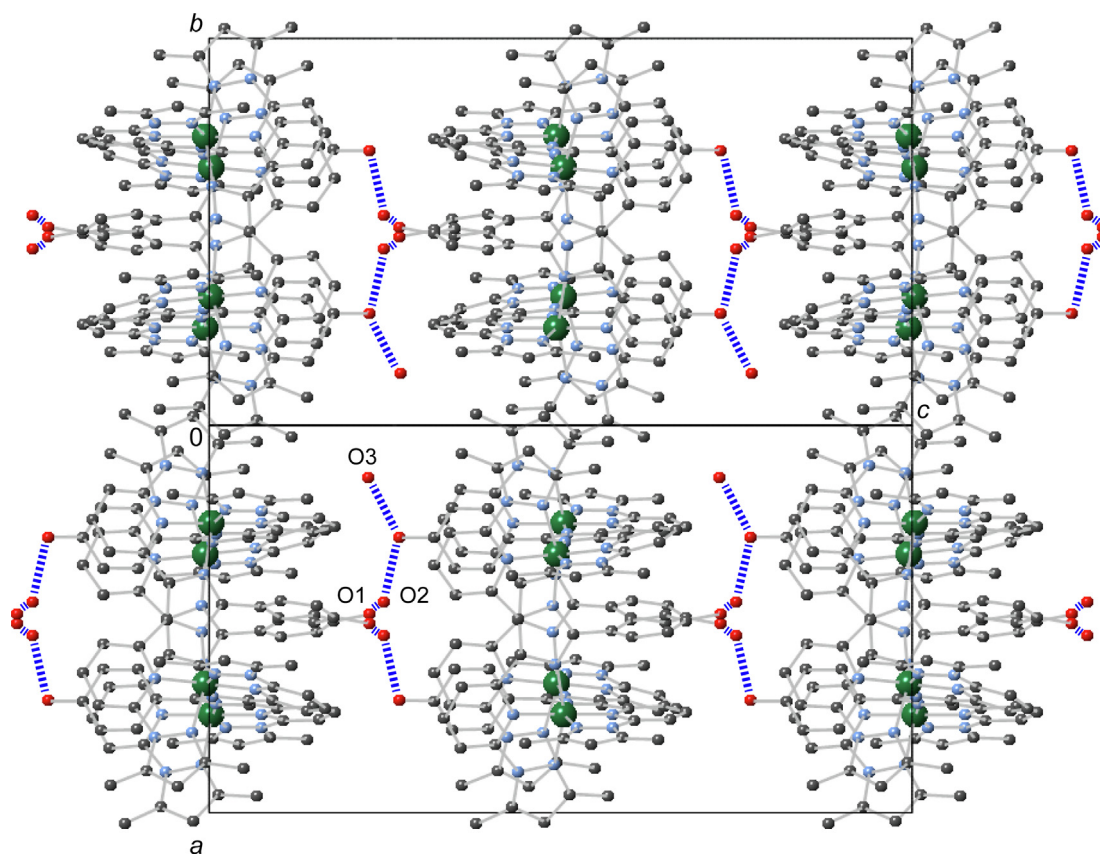
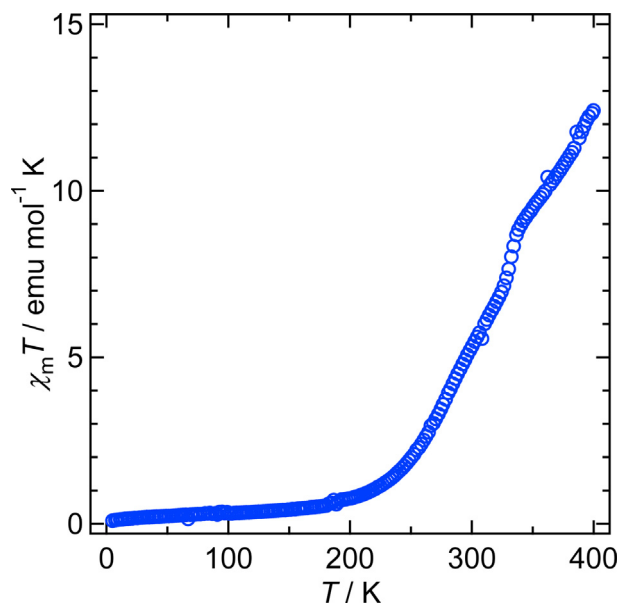**Fig. 2.** Packing structure of **1**. Hydrogen bonds are shown in dashed blue lines.

Fig. 3. Plot of $\chi_m T$ vs. T for **1**.

Fig. 4. Mössbauer spectrum for **1** at 20 K. Blue and black lines indicate fitting curves, the parameters of which are given in the text.

backbone of multinuclear SCO complexes can lead to significant knock-on effects to the switching properties due to intermolecular and packing effects. We are now exploring how the nature of the supramolecular chemistry and intermolecular cooperativity of multinuclear SCO clusters can be tuned and manipulated to effect multiple spin transitions on demand under conditions close to room temperature.
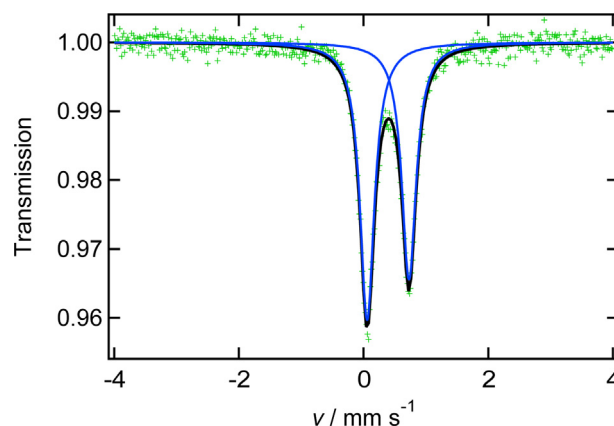
Appendix A. Supplementary data

Supplementary data to this article can be found online at https://doi.org/10.1016/j.jmmm.2019.03.101.

References

[1] P. Gütlich, H.A. Goodwin (Eds.), Spin Crossover in Transition Metal Compounds I, II, and III, Springer-Verlag, Berlin, Germany, 2004.

[2] (a) SCO review, H.S. Scott, R.W. Staniland, P.E. Kruger, Coord. Chem. Rev. 362 (2018) 24;
(b) A. Bousseksou, G. Molnár, L. Salmon, W. Nicolazzi, Chem. Soc. Rev. 40 (2011) 3313;
(c) M.A. Halcrow, Chem. Soc. Rev. 40 (40) (2011) 4119;
(d) J. Olguín, S. Brooker, Coord. Chem. Rev. 255 (2011) 203;
(e) P. Gütlich, Y. Garcia, H.A. Goodwin, Chem. Soc. Rev. 29 (29) (2000) 419;
(f) D.J. Harding, P. Harding, W. Phonsri, Coord. Chem. Rev. 313 (2016) 38;
(g) P. Guionneau, Dalton Trans. 43 (2014) 382;
(h) P. Gamez, J.S. Costa, M. Quesada, G. Aromí, Dalton Trans. 38 (2009) 7845.

[3] (a) Dinuclear SCO complexes, A. Bousseksou, G. Molnar, J.A. Real, K. Tanaka, Coord. Chem. Rev. 251 (2007) 1822;
(b) A.Y. Verat, N. Ould-Moussa, E. Jeanneau, B.L. Guennic, A. Bousseksou, S.A. Borshch, G.S. Matouzenko, Chem. Eur. J. 39 (2009) 10070;
(c) J.-L. Wang, Q. Liu, Y.-S. Meng, H. Zheng, H.-L. Zhu, Q. Shi, T. Liu, Inorg. Chem. 56 (2017) 10674;
(d) Y. Sunatsuki, H. Maruyama, K. Fujita, T. Suzuki, M. Kojima, N. Matsumoto, Bull. Chem. Soc. Jpn. 82 (2009) 1497;
(e) Y. Sunatsuki, R. Kawamoto, K. Fujita, H. Maruyama, T. Suzuki, H. Ishida, M. Kojima, S. Iijima, N. Matsumoto, Inorg. Chem. 48 (2009) 8784;
(f) K. Fujita, R. Kawamoto, R. Tsubouchi, Y. Sunatsuki, M. Kojima, S. Iijima, N. Matsumoto, Chem. Lett. 36 (2007) 1284;
(g) F. Tuna, M. Lees, G. Clarkson, M. Hannon, Chem. Eur. J. 10 (2004) 5737;
(h) Y. Garcia, C.M. Grunert, S. Reiman, O. van Campenhoudt, P. Gütlich, Eur. J. Inorg. Chem. (2006) 3333;
(i) A.R. Craze, N.F. Sciortino, M.M. Badbhade, C.J. Kepert, C.E. Marjo, F. Li, Inorganics 5 (2017) 62;
(j) D. Pelleteret, R. Clérac, C. Mathonière, E. Harté, W. Schmitt, P.E. Kruger, Chem. Commun. (2009) 221;
(k) R.J. Archer, C.S. Hawes, G.N.L. Jameson, V. McKee, B. Moubaraki, N.F. Chilton, K.S. urray, W. Schmitt, P.E. Kruger, Dalton Trans. 40 (2011) 12368;
(l) N. Struch, J.G. Brandenburg, G. Schnakenburg, N. Wagner, J. Beck, S. Grimme, A. Lützen, Eur. J. Inorg. Chem. (2015) 5503;
(m) S. Ohta, C. Yoshimura, N. Matsumoto, H. Okawa, A. Ohyoshi, Bull. Chem. Soc. Jpn. 59 (1986) 155.

[4] (a) A.B. Gasper, M.C. Muñoz, J.A. Real, J.A. Mater, Chem. 16 (2006) 2522;
(b) J.-F. Letard, C. Carbonera, J.A. Real, S. Kawata, S. Kaizaki, Chem. Eur. J. 15 (2009) 4146;
(c) S. Chorazy, R. Podgajny, K. Nakabayashi, J. Stanek, M. Rams, B. Siieklucka, S. Ohkoshi, Angew. Chem. Int. Ed. 54 (2015) 5093;
(d) J.J.M. Amoore, C.J. Kepert, J.D. Cashion, B. Moubaraki, S.M. Neville, K.S. Murray, Chem. Eur. J. 12 (2006) 8220;
(e) G.S. Matouzenko, E. Jeanneau, A.Y. Verat, A. Bousseksou, Dalton Trans. 40 (2011) 9608;
(f) I. Boldog, F.J. Muñoz-Lara, A.B. Gaspar, M.C. Muñoz, M. Seredyuk, J.A. Real,

Inorg. Chem. 48 (2009) 3710;
(g) M. Steinert, B. Schneider, S. Dechert, S. Demeshko, F. Meyer, Angew. Chem. Int. Ed. 53 (2014) 6135;
(h) N. Struch, C. Bannwarth, T.K. Ronson, Y. Lorenz, B. Mienert, N. Wagner, M. Engeser, E. Bill, R. Puttreddy, K. Rissanen, J. Beck, S. Grimme, J.R. Nitschke, A. Lützen, Angew. Chem. Int. Ed. 56 (2017) 4930;
(i) R.A. Bilbeisi, S. Zarra, H.L.C. Feltham, G.N.L. Jameson, J.K. Clegg, S. Brooker, J.R. Nitschke, Chem. Eur. J. 19 (2013) 8058;
(j) S. Samanta, S. Demesko, S. Dechert, F. Meyer, Angew. Chem. Int. Ed. 54 (2015) 583.

[5] (a) Molecular electronics, S. Sanvito, Chem. Soc. Rev. 40 (2011) 3336;
(b) J.M. Clemente-Juan, E. Coronado, A. Gaita-Ariño, Chem. Soc. Rev. 41 (2012) 7464.

[6] (a) Binuclear SCO systems by Real et al. J. Real, J. Zarembowitch, O. Kahn, X. Solans, Inorg. Chem. 26 (1987) 2939;
(b) J.A. Real, H. Bolvin, A. Bousseksou, A. Dworkin, O. Kahn, F. Varret, J. Zarembowitch, J. Am. Chem. Soc. 114 (1992) 4650;
(c) N.O. Moussa, E. Trzop, S. Mouri, S. Zein, G. Molnar, A.B. Gaspar, E. Collet, M.B.-L. Cointe, J.A. Real, S. Borshch, K. Tanaka, H. Cailleau, A. Bousseksou, Phys. Rev. B 75 (2007) 1.

[7] (a) Tetrahedral SCO tetranuclear cage complexes, D.-H. Ren, D. Qiu, C.-Y. Pang, Z. Li, Z.-G. Gu, Chem. Commun. 51 (2015) 788;
(b) A. Ferguson, M.A. Squire, D. Siretanu, D. Mitcov, C. Mathonière, R. Clérac, P.E. Kruger, Chem. Commun. 49 (2013) 1597;
(c) R.A. Bilbeisi, S. Zarra, H.L.C. Feltham, G.N.L. Jameson, J.K. Clegg, S. Brooker, J.R. Nitschke, Chem. Eur. J. 19 (2013) 7878;
(d) L. Li, N. Saigo, Y. Zhang, D.J. Fanna, N.D. Shepherd, J.K. Clegg, R. Zheng, S. Hayami, L.F. Lindoy, J.R. Aldrich-Wright, C.-G. Li, J.K. Reynolds, D.G. Harman, F. Li, J. Mater. Chem. C. 3 (2015) 7878.

[8] Octahedral cube-type SCO complexes, N. Struch, C. Bannwarth, T.K. Ronson, Y. Lorenz, B. Mienert, N. Wagner, M. Engeser, E. Bill, R. Puttreddy, K. Rissanen, J. Beck, S. Grimme, J.R. Nitschke, A. Lützen, Angew. Chem. Int. Ed. 56 (2017) 4930.

[9] E. Breuning, M. Ruben, J.-M. Lehn, F. Renz, Y. Garcia, V. Ksenofontov, P. Gutlich, E. Wegelius, K. Rissanen, [2 x 2] Grid SCO complex, Angew. Chem. Int. Ed. 39 (2000) 2504.

[10] D.-Y. Wu, O. Sato, Y. Einaga, C.-Y. Duan, [2 x 2] Grid SCO complex, Angew. Chem. Int. Ed. 48 (2009) 1475.

[11] B. Schneider, S. Demeshko, S. Dechert, F. Meyer, [2 x 2] Grid SCO complex, Angew. Chem. Int. Ed. 49 (2010) 9274.

[12] (a) T. Matsumoto, G.N. Newton, T. Shiga, S. Hayami, Y. Matsui, H. Okamoto, R. Kumai, Y. Murakami, H. Oshio, Nat. Commun. 5 (2014) 3865;
(b) T. Shiga, G.N. Newton, H. Oshio, Dalton Trans. 47 (2018) 7384;
(c) T. Shiga, Y. Sato, M. Tachibana, H. Sato, T. Matsumoto, H. Sagayama, R. Kumai, Y. Murakami, G.N. Newton, H. Oshio, Inorg. Chem. 57 (2018) 14013.

[13] (a) P. Guionneau, C. Brigouleix, Y. Barrans, A.E. Goeta, J.-F. Létard, J.A. Howard, J. Gaultier, D.C. Chasseau, C.R. Acad, Sci. Ser. IIc 4 (2001) 161;
(b) P. Guionneau, M. Marchivie, G. Bravic, J.F. Létard, D. Chasseau, Top. Curr. Chem. 234 (2004) 97.